PROCEEDINGS OF SCIENCE

Three loop amplitudes for V/H+jet production

Cesare Carlo Mella[a,*]

[a] *Physics Department, TUM School of Natural Sciences, Technical University of Munich, James-Franck-Straße 1, 85748, Garching, Germany*

E-mail: cesarecarlo.mella@tum.de

In this contribution, I will present the computation of the leading color three loop amplitude for the production of a vector boson and jet in Quantum Chromodynamics and recent developments in the computation of the three loop Feynman Integrals contributing to the leading color amplitude for Higgs and jet and to the three point Form Factor in $N = 4$ Super Yang Mills.

Loops and Legs in Quantum Field Theory (LL2024)
14-19, April, 2024
Wittenberg, Germany

*Speaker

PoS(LL2024)046

1. Introduction

Obtaining very precise predictions for processes in the Standard Model is essential for the success of the future LHC program. In the forthcoming High-Luminosity phase (HL-LHC), the expected increased luminosity of about 3 ab^{-1} for pp collisions will drastically decrease statistical uncertainties. The production of an electroweak vector boson (V) and a hadronic jet constitutes a precise probe of Quantum Chromodynamics (QCD), the theory that plays a fundamental role in hadronic collisions. Moreover, it is among the most precisely measured processes at LHC. In the case $V = Z, \gamma^*$, whose leptonic decay can be easily detected, experimental uncertainties for transverse momentum distributions are already below the percent level [1–5]. More differential observables, such as angular distributions of decay products, are also measured to a very high accuracy [6–8]. These allow for detailed studies of polarisation states of the vector boson, and its production mechanism. Given the astonishing precision of the experimental measurements, N^{3}LO predictions become necessary to perform phenomenological studies at high accuracy.
It is also hard to overestimate the importance of Higgs boson and jet production at the LHC. The Higgs boson has been at the center of both experimental and theoretical efforts since its discovery. By studying its properties, we aim to improve our understanding of electroweak symmetry breaking, the mechanism through which fermions and electroweak gauge bosons acquire mass. It is known that the Higgs cross-section receives large contributions from higher-order corrections [9, 10]. Therefore, N^{3}LO corrections are needed to reach the $O(1\%)$ level of accuracy [11].
In this context, scattering amplitudes are the bridge between the Standard Model and collider phenomenology. Their perturbative expansion requires the calculation of multiloops corrections. The amplitudes for vector boson plus jet production have been obtained up to two loops [12, 13], following the computation of the relevant master integrals [14, 15]. The same loop order is known for Higgs boson and jet production [16], in the heavy top quark mass limit, $m_T \to \infty$ [17–19]. Particular theoretical interest is reserved to the system formed by a Higgs and three gluons. The connection between the amplitude for this process and a three point Form Factor (FF) in $N = 4$ Super Yang-Mills (SYM) has been conjectured in [20, 21]. We are interested in investigating this at the three loop order.
In these proceedings, I will present progress towards the extension of these results to the three loop order and first results in the vector boson case. This requires the computation of the relevant three loop master integrals, including both planar and non-planar topologies. At this loop order, non-planar integrals bring a higher level of analytic complexity through the introduction of new *letters* in differential equation systems. Finally, we will stress how the reduction to a basis of master integrals poses a substantial computational challenge.

2. Computing an amplitude

We consider the decay of a particle with mass M^2 to three massless QCD partons, where the massive particle can be a Higgs boson or a vector boson. The production process is related to the decay through analytic continuation. We will generically indicate amplitudes with letter $\mathcal{M}$. We work in massless QCD with $N_f = 5$, where the top quark has been integrated out. In this theory,

PoS(LL2024)046

the Higgs couples to gluons through the effective interaction

$$\mathcal{L}_{int} = -\frac{\lambda}{4} H G_a^{\mu\nu} G_{a,\mu\nu}, \tag{1}$$

where $G_a^{\mu\nu}$ is the field strength tensor of the gluons and H is the Higgs field,. We are also interested in the three point Form Factor (FF) in $N = 4$ SYM,

$$\boldsymbol{F}_{O_2}(1,2,3,q) = \int d^D x\, e^{-\imath q\cdot x} \langle \Phi_1 \Phi_2 \Phi_3 | O_2(x) | 0 \rangle \,, \tag{2}$$

where $O_2 = \mathrm{tr}\left(\phi^2\right)$ is a Half-BPS operator of the theory, and Φ_i are three on-shell states. As we will explain later, the FF is closely related to the QCD amplitude for a system formed by a Higgs boson and three gluons.

2.1 Kinematics

We call the momenta of the three massless partons p_1, p_2, p_3, while p_4 is the momentum of the massive state. Mandelstam invariants are defined as

$$s_{12} = (p_1 + p_2)^2 \,, \qquad s_{13} = (p_1 + p_3)^2 \,, \qquad s_{23} = (p_2 + p_3)^2, \tag{3}$$

with all states outgoing. It is more convenient to work with the dimensionless ratios

$$x = \frac{s_{12}}{M^2}, \qquad y = \frac{s_{13}}{M^2}, \qquad z = \frac{s_{23}}{M^2}. \tag{4}$$

Momentum conservation implies

$$x + y + z = 1. \tag{5}$$

In the decay kinematic region, invariants are non-negative. This, together with (4), defines the kinematic region

$$x \geq 0, \qquad 0 \leq x \leq 1 - y, \qquad z = 1 - y - x. \tag{6}$$

2.2 Tensor decomposition

We decompose the QCD amplitudes in the most general basis of tensor structures compatible with external states and Lorentz invariance. We write

$$\mathcal{M} = \sum_{i=1}^{N} \mathcal{F}_i T_i \,, \tag{7}$$

where the N tensors $\{T_i\}$ contain all the dependence on external polarization states and the coefficients $\{F_i\}$, called *form factors*, are scalar functions of the Mandelstam invariants. Importantly, we work in 't Hooft-Veltman scheme and consider external states as four dimensional objects [22]. The polarization vector ϵ of an external gluon with momentum p satisfies the transversality conditions $p \cdot \epsilon = 0$. Using this and the choice of an axial gauge we can restrict the basis of tensor structures considerably. We then proceed defining a set of projectors $\{\mathcal{P}_i\}$ to extract the form factor. We assume

$$\mathcal{P}_i = \sum_{j=1}^{N} c_i^{(j)} T_j^\dagger \,, \tag{8}$$

PoS(LL2024)046

and fix the coefficients $c_i^{(j)}$ requiring that

$$\mathcal{P}_i \cdot \mathcal{M} \stackrel{!}{=} \mathcal{F}_i, \tag{9}$$

where the operation of the projection implies a sum over polarization states. Since the helicity amplitudes are linear combinations of the scalar form factors F_i, we can construct new projector operators, as linear combinations of the projectors P_i, that allow us to directly extract the helicity amplitudes for each helicity configuration [23]. We refer to [24, 25] for the explicit tensor decomposition and helicity amplitudes projectors for all processes we are interested in: $V \to q\bar{q}g$, $V \to ggg$, $H \to q\bar{q}g$, $H \to ggg$.

2.3 Computational setup

For what concerns the QCD amplitudes, at a fixed loop order, we generate all relevant Feynman diagrams using QGRAF [26]. We insert Feynman rules and perform projection onto helicity amplitudes in FORM [27]. Each projected contribution is written as a linear combination of Feynman Integrals with coefficients that are rational functions of the invariants and of the space-time dimension D. On the other side, the integrand for the FF in Eq (2) has been determined by using generalized unitarity methods to constrain an ansatz satisfying relations from color-kinematic duality [28]. As for the QCD amplitudes, also in this case one can decompose the integrand as a linear combination of Feynman integrals which we map to auxiliary topologies using REDUZE [29]. Feynman integrals can be generally written as

$$I = \int \left(\prod_{l=1}^{L} (-M_H^2)^{-\epsilon} e^{\gamma_E \epsilon} \frac{\mathrm{d}^D k_l}{i\pi^{d/2}} \right) \prod_{i=1}^{N_p} D_i^{-a_i} \,, \tag{10}$$

where k_l are the L loop momenta, D_i the propagators raised to integer powers a_i, N_p is the number of such propagators, and $\gamma_E = 0.577\ldots$ the Euler-Mascheroni constant. The topology of each scalar integral is uniquely identified by the propagators which appear in the denominator. The scalar integrals defined in (10) satisfy integration-by-parts (IBP) identities [30, 31]. Therefore, we can express them in terms of a smaller set of master integrals.

To evaluate the master integrals, we use the method of differential equations [32–35]. We build a so called canonical basis [36] for the master integrals, in which the dependence on the dimensional regulator $\epsilon = \frac{4-D}{2}$ is factorized form kinematics in the differential equation.

3. The Leading Color (LC) amplitude for $Vq\bar{q}g$

Following the procedure outlined in the previous section, we computed the three loop helicity amplitudes for the decay of a vector boson into a quark-antiquark pair and a gluon in the leading color

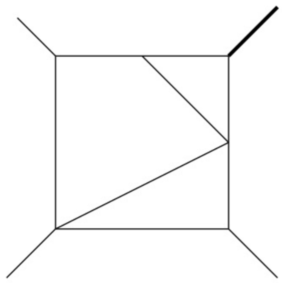

Figure 1: 8 propagator topology whose symbol solution violates the non-adjacency conjecture.

approximation, [37]. In fact, the three loop amplitude $\mathcal{M}^{(3)}$ admits the following decomposition

$$
\begin{aligned}
\mathcal{M}^{(3)} = {} & N^3\,\Omega_1^{(3)} + N\Omega_2^{(3)} + \frac{1}{N}\Omega_3^{(3)} + \frac{1}{N^3}\Omega_4^{(3)} \\
& + N_f\,N^2\Omega_5^{(3)} + N_f\Omega_6^{(3)} + \frac{N_f}{N^2}\Omega_7^{(3)} \\
& + N_f^2 N\,\Omega_8^{(3)} + \frac{N_f^2}{N}\Omega_9^{(3)} + N_f^3\Omega_{10}^{(3)} \\
& + N_{f,V}N^2\Omega_{11}^{(3)} + N_{f,V}\Omega_{12}^{(3)} \\
& + \frac{N_{f,V}}{N^2}\Omega_{13}^{(3)} + N_f N_{f,V} N\Omega_{14}^{(3)} + \frac{N_f N_{f,V}}{N}\Omega_{15}^{(3)},
\end{aligned}
\tag{11}
$$

where N is the number of colors, N_f is the number of flavors and $N_{f,V}$ refers to the contribution where the vector boson couples to an internal fermion loop. We assume N and N_f of the same size and compute only the leading terms of the expansion: N^3, N^2N_f, N_f^2N, N_f^3. Importantly, the leading color for V+jet receives contribution only from planar integrals. Planar topologies were investigated in [38, 39], where a solution was given up to order ϵ^6 in terms of multiple polylogarithms (MPLs) [14, 40–42] with alphabet

$$
\vec{\alpha} = \{x, y, 1-x, 1-y, x+y, 1-x-y\}. \tag{12}
$$

This is the same alphabet which appears in the corresponding 2-loop calculation, and we refer to it as the 2-loop alphabet. We used KIRA2 [43, 44] to perform IBP reduction of integrals up to rank 5. This was computationally expensive, with very high memory usage of the order of 1 TB.

We verified that the symbol[1] of the leading color $Vgq\bar{q}$ amplitude satisfies the conjectured non-adjacency conditions [46, 47], even though integrals whose symbol is not satisfying the conjecture were found in one of the so-called tennis-court topology [48]. In particular, a single subsector with 8 propagators is identified as the source of this violation. This integral is drawn in Figure 1.

We have performed analytic continuation of all helicity amplitudes to all production regions: $q\bar{q} \to Vg$, $gq \to Vq$, $g\bar{q} \to V\bar{q}$.

[1]See for example [45] for an introduction to the symbol concept with an application to the $H \to ggg$ at 2-loop.

4. Towards the $H \rightarrow ggg$ amplitude and the $N = 4$ Form Factor at 3 loop in leading color approximation

The amplitude for the process $H \rightarrow ggg$ with QCD corrections and the FF in $N = 4$ SYM defined in Eq (2) are closely related. It has been verified up to 2 loop that some of the properties of the FF are in fact inherited by the QCD counterpart, see 4.3. Besides planar topologies, the leading color amplitude for Higgs and three gluons and the FF receive contributions also from non-planar topologies. The five irreducible non-planar top sectors that contribute are drawn in Figure 2. The two main tasks we must face are

- Find a canonical basis for all the top sectors and provide a solution for the integrals.
- Perform IBP reduction to master integrals.

4.1 Finding canonical basis

As anticipated in Section 2, we use the differential equation method to compute master integrals. In general, for a master integral basis $\vec{I}$, the differential equation system will be written in the form

$$d\vec{I} = A(s_{ij}, \epsilon) \cdot \vec{I}. \tag{13}$$

It was shown in [36] that transformations T to a new basis $\vec{J} = T \cdot \vec{I}$ can be found such that the differential equation in the new basis system assumes the particular form

$$d\vec{J} = \epsilon \tilde{A}(s_{ij}) \cdot \vec{J}, \tag{14}$$

where the ϵ dependence factorises. Moreover, the connection matrix $\tilde{A}$ has entries that are $d\log$ forms. We write,

$$\tilde{A}(s_{ij}) = \sum_{i=1}^{N_L} A_i \, d\log \alpha_i, \tag{15}$$

where the $\{A_i\}$ are matrices of rational numbers, the $\{\alpha_i\}$, called *letters*, are algebraic functions of the invariants and N_L is the number of letters.

The first topology in Figure 2 was already addressed in [48]. A canonical basis was found and a solution was given for all the integrals in terms of MPLs. The alphabet for this topology is bigger than for the planar case. In particular, 2 quadratic letters appear on top of the linear 2-loop alphabet of Eq (12). We are interested in finding the canonical basis for all the remaining topologies in Figure 2. Working at the differential equation level and looking for a transformation matrix T that realizes the ϵ-factorised form is, in general, a very hard task. Better approaches aim at finding canonical candidates before the differential equation construction. A number of techniques have been developed to address this problem: most of them are based on the conjectural property of canonical candidates that they can be written at the integrand level in $d\log$ form with constant leading singularity [49]. Finding such candidates is most easily done working in Baikov representation and, in particular, in the simplified loop-by-loop construction [50]. In Baikov representation, a Feynman integral F whose graph has m propagators has the following schematic form,

$$F \propto \int_C \frac{dz_1 \cdots dz_n}{z_{t_1} \cdots z_{t_m}} P^{\frac{D-L-E-1}{2}}, \tag{16}$$

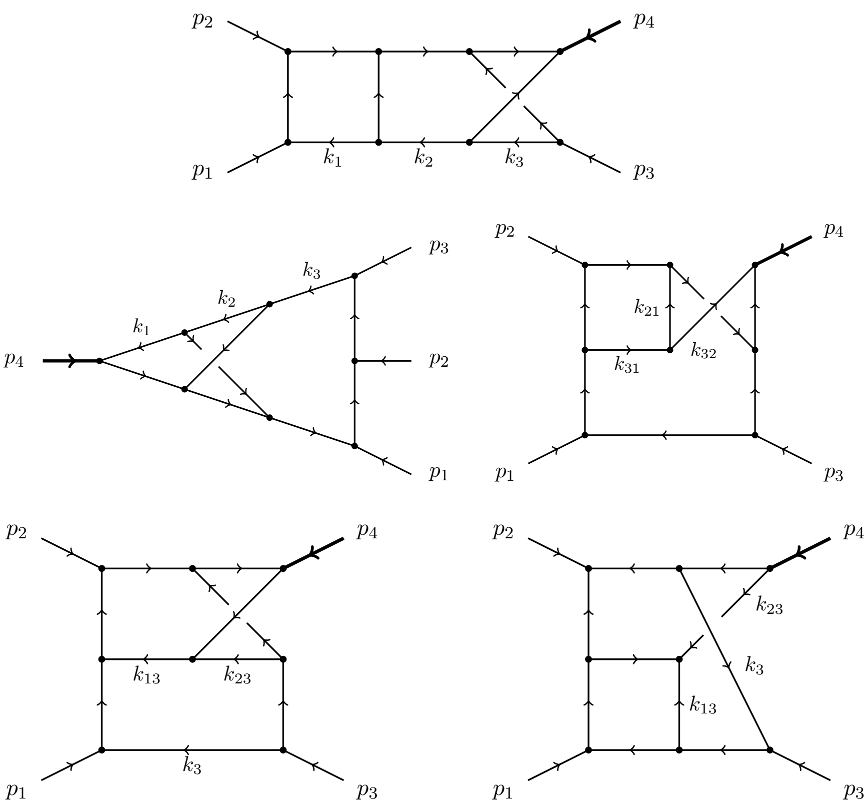

Figure 2: Irreducible non planar top sectors contributing to the leading color of $H \to ggg$ and the $\mathrm{tr}(\phi^2)$ Form Factor.

where n is the total number of propagators in the auxiliary topology, L is the number of loops, E is the number of independent external momenta and $P = P(\{s_{ij}\}, \{z_i\})$ is the Baikov polynomial. The Baikov polynomial is defined as the Gram determinant of all the external and loop momenta. A candidate C is built by multiplying the integrand with a polynomial ansatz N,

$$C \propto \int_C \frac{dz_1 \cdots dz_n}{z_{t_1} \cdots z_{t_m}} P^{\frac{D-L-E-1}{2}} N(\{c_j\}). \tag{17}$$

Numerators are of the general form,

$$N(\{c_j\}) = \sum_j c_j \prod_{k \in S_j} z_k, \tag{18}$$

where the set S_j is a set of propagator indices and we leave the sum over j unspecified, to stress that the dimensions of the ansatz cannot be determined in advance. One should fix the coefficients $\{c_j\}$ in such a way that the aforementioned $d\log$ form is obtained. The analysis is usually performed on various propagator cuts, rather than on the full integrand. Baikov representation turns out to be particularly suited for the job, given that the cut operation is obtained by taking the corresponding residues in the integration variables. Summarizing our strategy, we built all canonical basis employing the following techniques:

- We used the automated package DLogBasis [51] for sectors with a low number of propagators. Moreover, simple integrals like bubbles with doubled propagators are known to be canonical, [52]. We used this information when possible.
- For higher sectors, and in particular for top sectors, we performed a leading singularity analysis on the cuts.
- In one case, a close-to-canonical form of the differential equation was achieved. A final basis rotation was performed at the level of the differential equation matrix.

From the canonical differential equations, we can read off the alphabet

$$\begin{aligned}\vec{\alpha} =&\{\alpha_1, \ldots, \alpha_{20}\} = \\ &\Big\{x, y, 1-x-y, 1-x, 1-y, x+y, \frac{(1-x-y)x-\sqrt{-x(1-x-y)y}}{(1-x-y)x+\sqrt{-x(1-x-y)y}}, \\ &\frac{xy-\sqrt{-x(1-x-y)y}}{xy+\sqrt{-x(1-x-y)y}}, 1-y\,(1+x)\,, 1-x\,(1+y)\,, y^2+x-y, \\ &x^2+y-x, -y+(1-x)^2\,, (x+y)^2-y, (x+y)^2-x, (y-1)^2-x, \\ &y^2+xy+x, x^2+xy+y, (y-1)^2+xy, (x-1)^2+xy\Big\},\end{aligned} \tag{19}$$

where the variables are defined as in (4). The alphabet consists of 20 letters: 2 of them are associated with a square root, 12 are quadratic letters and the rest is the 2 loop alphabet. We stress that although rationalization of the square root is possible, it turns out to be difficult to rationalize the root while keeping the rest of the alphabet at most quadratic.

4.2 Boundary conditions and symbol solution

We write the solution of the differential equation as an expansion in ϵ

$$\vec{J}(x,y) = \sum_n \epsilon^n \vec{J}^{(n)}(x,y), \tag{20}$$

which is obtained in terms of iterated integrals, via Eq. (14). We normalize the basis such that the expansion starts at order ϵ^0, which is easily verified as being constant, $\vec{J}^{(0)}(x,y) = \vec{J}^{(0)}$. The solution at order ϵ^n, $\vec{J}^{(n)}$, is called the weight-n part of the solution.
It is possible to fix the boundary conditions using information from the analytic properties of Feynman integrals. The only physical thresholds in our problem are identified by the letters $\{\alpha_1, \alpha_2, \alpha_3\}$. The singular behavior close to a threshold can be predicted from the differential equation. For example, suppose we are interested in studying the behavior of the solution for $x \to 0$. The differential equation simplifies to the form

$$\frac{\partial \vec{J}}{\partial x} \sim \frac{\epsilon}{x} A_x \vec{J}, \tag{21}$$

and a solution is obtained by exponentiation of the numerical matrix A_x

$$\vec{J}(x \to 0, y) = x^{\epsilon A_x} \vec{J}_0(y), \tag{22}$$

with J_0 a vector of function of the other variable y only (and ϵ). The matrix exponential will contain terms of the form $x^{a\epsilon}$, with a positive or negative. It was argued in [51] that positive a are associated with logarithmic divergences of UV type, which cannot appear since our basis is UV finite. Requiring the absence of such divergences and imposing regularity of the solution on the rest of the alphabet, $\{\alpha_4, \cdots, \alpha_{20}\}$, which is not associated to any physical singular behaviour, we can determine boundary constants for all master integrals in a full analytic manner, given the knowledge of single-scale integrals only.
The constant weight-0 solution, $O(\epsilon^0)$, is fully determined by the boundary constants at that order. With the weight zero solution at hand, we determined the symbol level solution, which contains the information about the function appearing at different weights, while retaining only the weight-0 boundary constants. By inspecting the symbol solution, we know that quadratic letters and square root letters start contributing from $O(\epsilon^4)$.

4.3 $N = 4$ Form Factor at symbol level

We consider now the three point Form Factor in Eq (2). The symbol level solution for it has been recently bootstrapped up to eight loops [53]. The result has the following properties:

- It is of uniform transcendental weight;
- The finite remainder is of maximum transcendental weight;
- Only the 2 loop letters $\{\alpha_1, \ldots, \alpha_6\}$ contribute up to eight loops.

As a strong check of the calculation, we reproduced the 3 loop symbol level result of [53] by performing IBP reduction of the integrand to our canonical basis and inserting the symbol solutions for the master integrals. For the FF, we required the reduction of integrals up to rank 2. This is considerably easier than the QCD counterpart, where a reduction of non-planar integrals up to rank 6 is needed. At present, such a reduction to master integrals is not available. It has been conjectured, and verified up to two loops, that the highest transcendental part of the $H \to ggg$ amplitude is captured entirely by the FF. If this conjecture is verified also at three loop, it implies that only the 2-loop alphabet contributes to the highest transcendental part of the amplitude. This would indicate that the finite remainder for this amplitude might be simpler than expected, at least from the point of view of the functional basis in which it can be written.

5. Conclusion

In this contribution, I described the computation of the leading color V+jet amplitude in the $q\bar{q}$ channel at the three-loop order. I also described recent progress toward the calculation of the leading color three loop H+jet amplitude and Form Factor in $N = 4$ SYM. I focused on the procedure to build a canonical basis for all the required master integrals and I showed how the knowledge of analytic properties of Feynman integrals can be used to fix the boundary constants. A full solution for the master integrals and IBP reduction for the H+jet amplitude remain the two outstanding tasks to be addressed in the future.

PoS(LL2024)046

6. Acknowledgements

I wish to thank my collaborators William J.T. Bobadilla, Thomas Gehrmann, Johannes M. Henn, Petr Jakubčík, Jungwon Lim, Nikolaos Syrrakos, Lorenzo Tancredi, working on the project that inspired this contribution. My research is supported by the Excellence Cluster ORIGINS funded by the Deutsche Forschungsgemeinschaft (DFG, German Research Foundation) under Germany's Excellence Strategy – EXC-2094-390783311.

References

[1] ATLAS collaboration, *Measurement of the Z/γ^* boson transverse momentum distribution in pp collisions at $\sqrt{s} = 7$ TeV with the ATLAS detector*, JHEP **09** (2014) 145 [1406.3660].

[2] CMS collaboration, *Measurement of the Z boson differential cross section in transverse momentum and rapidity in proton–proton collisions at 8 TeV*, Phys. Lett. B **749** (2015) 187 [1504.03511].

[3] CMS collaboration, *Measurement of the Rapidity and Transverse Momentum Distributions of Z Bosons in pp Collisions at $\sqrt{s} = 7$ TeV*, Phys. Rev. D **85** (2012) 032002 [1110.4973].

[4] ATLAS collaboration, *Measurement of the transverse momentum and ϕ^*_η distributions of Drell–Yan lepton pairs in proton–proton collisions at $\sqrt{s} = 8$ TeV with the ATLAS detector*, Eur. Phys. J. C **76** (2016) 291 [1512.02192].

[5] LHCb collaboration, *Measurement of the forward Z boson production cross-section in pp collisions at $\sqrt{s} = 7$ TeV*, JHEP **08** (2015) 039 [1505.07024].

[6] CMS collaboration, *Measurement of the weak mixing angle with the Drell-Yan process in proton-proton collisions at the LHC*, Phys. Rev. D **84** (2011) 112002 [1110.2682].

[7] ATLAS collaboration, *Measurement of the forward-backward asymmetry of electron and muon pair-production in pp collisions at $\sqrt{s} = 7$ TeV with the ATLAS detector*, JHEP **09** (2015) 049 [1503.03709].

[8] LHCb collaboration, *Measurement of the forward-backward asymmetry in $Z/\gamma^* \to \mu^+\mu^-$ decays and determination of the effective weak mixing angle*, JHEP **11** (2015) 190 [1509.07645].

[9] S. Dawson, *Radiative corrections to Higgs boson production*, Nucl. Phys. B **359** (1991) 283.

[10] M. Spira, A. Djouadi, D. Graudenz and P.M. Zerwas, *Higgs boson production at the LHC*, Nucl. Phys. B **453** (1995) 17 [hep-ph/9504378].

[11] F. Caola, W. Chen, C. Duhr, X. Liu, B. Mistlberger, F. Petriello, G. Vita and S. Weinzierl, *The Path forward to N^{3}LO*, in *2022 Snowmass Summer Study*, 3, 2022 [2203.06730].

[12] L.W. Garland, T. Gehrmann, E.W.N. Glover, A. Koukoutsakis and E. Remiddi, *Two loop QCD helicity amplitudes for $e^+e^- \to 3$ jets*, *Nucl. Phys. B* **642** (2002) 227 [hep-ph/0206067].

[13] T. Gehrmann, T. Peraro and L. Tancredi, *Two-loop QCD corrections to the $V \to q\bar{q}g$ helicity amplitudes with axial-vector couplings*, *JHEP* **02** (2023) 041 [2211.13596].

[14] T. Gehrmann and E. Remiddi, *Two loop master integrals for $\gamma^* \to 3$ jets: The Planar topologies*, *Nucl. Phys.* **B601** (2001) 248 [hep-ph/0008287].

[15] T. Gehrmann and E. Remiddi, *Two loop master integrals for $\gamma^* \to 3$ jets: The Nonplanar topologies*, *Nucl. Phys.* **B601** (2001) 287 [hep-ph/0101124].

[16] T. Gehrmann, M. Jaquier, E.W.N. Glover and A. Koukoutsakis, *Two-loop QCD corrections to the helicity amplitudes for $H \to 3$ partons*, *Journal of High Energy Physics* **2012** (2012) .

[17] F. Wilczek, *Decays of heavy vector mesons into higgs particles*, *Phys. Rev. Lett.* **39** (1977) 1304.

[18] M. Shifman, A. Vainshtein and V. Zakharov, *Remarks on higgs-boson interactions with nucleons*, *Physics Letters B* **78** (1978) 443.

[19] T. Inami, T. Kubota and Y. Okada, *Effective Gauge Theory and the Effect of Heavy Quarks in Higgs Boson Decays*, *Z. Phys. C* **18** (1983) 69.

[20] A.V. Kotikov and L.N. Lipatov, *DGLAP and BFKL equations in the $N = 4$ supersymmetric gauge theory*, *Nucl. Phys. B* **661** (2003) 19 [hep-ph/0208220].

[21] A.V. Kotikov, L.N. Lipatov, A.I. Onishchenko and V.N. Velizhanin, *Three loop universal anomalous dimension of the Wilson operators in $N = 4$ SUSY Yang-Mills model*, *Phys. Lett. B* **595** (2004) 521 [hep-th/0404092].

[22] T. Peraro and L. Tancredi, *Tensor decomposition for bosonic and fermionic scattering amplitudes*, *Phys. Rev. D* **103** (2021) 054042 [2012.00820].

[23] T. Peraro and L. Tancredi, *Physical projectors for multi-leg helicity amplitudes*, *JHEP* **07** (2019) 114 [1906.03298].

[24] T. Gehrmann, P. Jakubčík, C.C. Mella, N. Syrrakos and L. Tancredi, *Two-loop helicity amplitudes for H+jet production to higher orders in the dimensional regulator*, *JHEP* **04** (2023) 016 [2301.10849].

[25] T. Gehrmann, P. Jakubčík, C.C. Mella, N. Syrrakos and L. Tancredi, *Two-loop helicity amplitudes for V+jet production including axial vector couplings to higher orders in ϵ*, *JHEP* **09** (2023) 192 [2306.10170].

[26] P. Nogueira, *Automatic Feynman graph generation*, *J. Comput. Phys.* **105** (1993) 279.

[27] J.A.M. Vermaseren, *New features of FORM*, math-ph/0010025.

[28] G. Lin, G. Yang and S. Zhang, *Full-color three-loop three-point form factors in N = 4 SYM*, *JHEP* **03** (2022) 061 [2111.03021].

[29] C. Studerus, *Reduze-Feynman Integral Reduction in C++*, *Comput. Phys. Commun.* **181** (2010) 1293 [0912.2546].

[30] K.G. Chetyrkin and F.V. Tkachov, *Integration by Parts: The Algorithm to Calculate beta Functions in 4 Loops*, *Nucl. Phys. B* **192** (1981) 159.

[31] S. Laporta, *High precision calculation of multiloop Feynman integrals by difference equations*, *Int. J. Mod. Phys. A* **15** (2000) 5087 [hep-ph/0102033].

[32] A.V. Kotikov, *Differential equations method: New technique for massive Feynman diagrams calculation*, *Phys. Lett. B* **254** (1991) 158.

[33] A.V. Kotikov, *Differential equations method: The Calculation of vertex type Feynman diagrams*, *Phys. Lett. B* **259** (1991) 314.

[34] A.V. Kotikov, *Differential equation method: The Calculation of N point Feynman diagrams*, *Phys. Lett. B* **267** (1991) 123.

[35] T. Gehrmann and E. Remiddi, *Differential equations for two loop four point functions*, *Nucl. Phys. B* **580** (2000) 485 [hep-ph/9912329].

[36] J.M. Henn, *Multiloop integrals in dimensional regularization made simple*, *Phys. Rev. Lett.* **110** (2013) 251601 [1304.1806].

[37] T. Gehrmann, P. Jakubčík, C.C. Mella, N. Syrrakos and L. Tancredi, *Planar three-loop QCD helicity amplitudes for V+jet production at hadron colliders*, *Phys. Lett. B* **848** (2024) 138369 [2307.15405].

[38] D.D. Canko and N. Syrrakos, *Planar three-loop master integrals for 2 → 2 processes with one external massive particle*, *JHEP* **04** (2022) 134 [2112.14275].

[39] S. Di Vita, P. Mastrolia, U. Schubert and V. Yundin, *Three-loop master integrals for ladder-box diagrams with one massive leg*, *JHEP* **09** (2014) 148 [1408.3107].

[40] A.B. Goncharov, *Multiple polylogarithms, cyclotomy and modular complexes*, *Math. Res. Lett.* **5** (1998) 497 [1105.2076].

[41] E. Remiddi and J. Vermaseren, *Harmonic polylogarithms*, *Int.J.Mod.Phys.* **A15** (2000) 725 [hep-ph/9905237].

[42] J. Vollinga and S. Weinzierl, *Numerical evaluation of multiple polylogarithms*, *Comput.Phys.Commun.* **167** (2005) 177 [hep-ph/0410259].

[43] P. Maierhöfer, J. Usovitsch and P. Uwer, *Kira—A Feynman integral reduction program*, *Comput. Phys. Commun.* **230** (2018) 99 [1705.05610].

[44] J. Klappert, F. Lange, P. Maierhöfer and J. Usovitsch, *Integral reduction with Kira 2.0 and finite field methods*, Comput. Phys. Commun. **266** (2021) 108024 [2008.06494].

[45] C. Duhr, *Hopf algebras, coproducts and symbols: an application to Higgs boson amplitudes*, *JHEP* **08** (2012) 043 [1203.0454].

[46] L.J. Dixon, A.J. McLeod and M. Wilhelm, *A Three-Point Form Factor Through Five Loops*, *JHEP* **04** (2021) 147 [2012.12286].

[47] D. Chicherin, J.M. Henn and G. Papathanasiou, *Cluster algebras for Feynman integrals*, Phys. Rev. Lett. **126** (2021) 091603 [2012.12285].

[48] J.M. Henn, J. Lim and W.J. Torres Bobadilla, *First look at the evaluation of three-loop non-planar Feynman diagrams for Higgs plus jet production*, 2302.12776.

[49] N. Arkani-Hamed, J.L. Bourjaily, F. Cachazo and J. Trnka, *Local Integrals for Planar Scattering Amplitudes*, *JHEP* **06** (2012) 125 [1012.6032].

[50] H. Frellesvig and C.G. Papadopoulos, *Cuts of Feynman Integrals in Baikov representation*, *JHEP* **04** (2017) 083 [1701.07356].

[51] J. Henn, B. Mistlberger, V.A. Smirnov and P. Wasser, *Constructing d-log integrands and computing master integrals for three-loop four-particle scattering*, *JHEP* **04** (2020) 167 [2002.09492].

[52] W. Flieger and W.J. Torres Bobadilla, *Landau and leading singularities in arbitrary space-time dimensions*, 2210.09872.

[53] L.J. Dixon, O. Gurdogan, A.J. McLeod and M. Wilhelm, *Bootstrapping a stress-tensor form factor through eight loops*, *JHEP* **07** (2022) 153 [2204.11901].